AD-A061 822 ROYAL AIRCRAFT ESTABLISHMENT FARNBOROUGH (ENGLAND) F/G 17/8
SOME CHARACTERISTICS OF THE PARTICLES USED IN LASER ANEMOMETRY --ETC (U)
MAY 78 P R SHARPE

UNCLASSIFIED RAE-TR-78055 DRIC-BR-64224 NL

| OF |
AD
A061822

END
DATE
FILMED
2 79
DDC

ROYAL AIRCRAFT ESTABLISHMENT

*

(9) Technical Report 78055

(11) May 1978

(6) SOME CHARACTERISTICS OF THE PARTICLES USED IN LASER ANEMOMETRY APPLICATIONS AT RAE (7)

by

(10) P.R. Sharpe

(12) 40 p.

*

Procurement Executive, Ministry of Defence
Farnborough, Hants

REPORT DOCUMENTATION PAGE

Overall security classification of this page

UNCLASSIFIED

As far as possible this page should contain only unclassified information. If it is necessary to enter classified information, the box above must be marked to indicate the classification, e.g. Restricted, Confidential or Secret.

1. DRIC Reference (to be added by DRIC)	2. Originator's Reference	3. Agency Reference	4. Report Security Classification/Marking
	RAE TR 78055	N/A	UNCLASSIFIED

5. DRIC Code for Originator	6. Originator (Corporate Author) Name and Location
850100	Royal Aircraft Establishment, Farnborough, Hants, UK
5a. Sponsoring Agency's Code	6a. Sponsoring Agency (Contract Authority) Name and Location
N/A	N/A

7. Title: Some characteristics of the particles used in laser anemometry applications at RAE

7a. (For Translations) Title in Foreign Language

7b. (For Conference Papers) Title, Place and Date of Conference

8. Author 1. Surname, Initials	9a. Author 2	9b. Authors 3, 4	10. Date	Pages	Refs.
Sharpe, P.R.			May 1978		27

11. Contract Number	12. Period	13. Project	14. Other Reference Nos.
N/A	N/A		IT 158

15. Distribution statement

(a) Controlled by – Unlimited (Memo)

(b) Special limitations (if any) –

16. Descriptors (Keywords) (Descriptors marked * are selected from TEST)

Anemometry (laser Doppler). Particle sizing.

17. Abstract

A knowledge of some of the characteristics, for example the mean diameter, of the particles used in laser anemometry experiments is of considerable importance if the results obtained are to be interpreted with confidence. Problems associated with the determination of this quantity are discussed, relevant aspects of the scattering of light by spherical particles are briefly summarised and the results of some laboratory experiments are presented. It is shown that the seeding technique used at present, based on a commercial oil-mist generator, gives satisfactory results for most laser anemometry applications of interest to RAE.

F 5910/1

RAE Form A143

UDC 533.6.082.5 : 539.215.4

ROYAL AIRCRAFT ESTABLISHMENT

Technical Report 78055

Received for printing 22 May 1978

SOME CHARACTERISTICS OF THE PARTICLES USED IN LASER ANEMOMETRY APPLICATIONS AT RAE

by

P. R. Sharpe

SUMMARY

A knowledge of some of the characteristics, for example the mean diameter, of the particles used in laser anemometry experiments is of considerable importance if the results obtained are to be interpreted with confidence. Problems associated with the determination of this quantity are discussed, relevant aspects of the scattering of light by spherical particles are briefly summarised and the results of some laboratory experiments are presented. It is shown that the seeding technique used at present, based on a commercial oil-mist generator, gives satisfactory results for most laser anemometry applications of interest to RAE.

Departmental Reference: IT 158

LIST OF CONTENTS

1 INTRODUCTION

The laser anemometer is an instrument for measuring the dynamic properties of fluid motion. It is based on the Doppler effect at optical frequencies and uses the information contained in the temporal variations of the light scattered by particles embedded in the fluid. It offers the fluid dynamicist the capability of making essentially non-intrusive studies of flow situations which were previously either very difficult or impossible to carry out[1].

Early laser anemometry measurements at RAE were made in naturally seeded flows[2]. However, since naturally occurring particles can vary widely in their characteristics, including size, it is desirable to start with an unseeded flow and to add to it particles with known characteristics.

In the closed circuit wind tunnels at RAE in which experiments have been carried out it has been found that the air becomes relatively clean after a short running time. Consequently it only remains to choose a suitable material and an appropriate method of generating seeding particles from it. There are several important factors to be considered in making this choice:

(i) If the particles are to convey meaningful velocity information about the flow, they must faithfully reproduce the motion of the fluid element in which they are embedded, even when this experiences strong forces; for example when traversing a shock wave or following a turbulent wake. There is a large amount of literature on this subject, but there are still some topics which are only partially understood; for example, particle behaviour in a rotating and/or turbulent flow. Boothroyd[3] gives a general review of the subject whilst Karchmer[4] and Kirsch and Mazumder[5] deal with oscillating flows. Some workers use the behaviour of the particle in strongly accelerating flows to obtain an estimate of its size; see for example Refs 6-8. The conclusions reached in these studies indicate that the particles should be made as small as possible, consistent with the requirement that they do not exhibit any Brownian motion in response to the motion of the gas molecules.

(ii) The light backscattered from the particle must be sufficiently strong to make experiments possible in the larger wind tunnels. Clearly for the particle to scatter any light, its refractive index must be different from that of the host fluid. The size of the particle also affects the scattering efficiency.

(iii) Toxicity, abrasiveness, cost and ease of generation should also be taken into account.

Oil droplets with diameters in the range 0.1-1.0 micron meet these criteria for most practical applications of interest to RAE. The seeding method adopted during the laser anemometry development programme at RAE is based on a commercial oil-mist generator, designed to produce a fine oil mist suitable for use in lubrication systems. Oil consumption is found to be, typically, approximately 2 ml per hour. No serious problems arising from wind-tunnel contamination have been encountered.

A variety of experiments have now been carried out using this form of seeding; of particular interest to studies of particle behaviour in rapidly accelerating flows and to the overall accuracy attainable were measurements made in supersonic flow over a ten-degree cone at normal incidence[9]. The results of this experiment could be compared with theoretical calculations of the velocity distribution, for a given stagnation temperature and Mach number. Experience has also been gained in the 3ft × 3ft supersonic wind tunnel at RAE, Bedford; studies of the interaction of a normal shock wave with a turbulent boundary layer gave quantitative results[1,10] which accorded with theoretical expectations and in regions where no fully detailed theoretical prediction was available, new information was obtained.

Although these experiments have verified the predicted particle behaviour an independent laboratory study of some of the particle characteristics was carried out. The main quantities of interest were the refractive index and the mean diameter of the droplets produced by the oil-mist generator. A specification of the oil is given in Ref 11.

A widely used method for the determination of the size of a small, spherical, dielectric particle is based on measurements of the light scattered by the particle out of an incident beam. Experiments were carried out to determine the refractive index of the oil and the angular distribution of the scattered light field for a particular wavelength and direction of polarisation of the incident light; the effect of a settling chamber was also studied. Finally an attempt was made to verify the value of the size derived from the results of the angular scattering experiment by measurement of the turbidity of the oil mist at several different wavelengths.

This Report outlines the basic theory of light scattering applied to small, spherical particles and describes the experiments carried out on the oil droplets. 055

2 THEORY OF LIGHT SCATTERING

2.1 Mie theory

Light scattering experiments can be used to characterise small dielectric spheres since the measurable quantities are connected by exact theoretical relationships. The original formulation of these relationships is due to Lorenz[12] although they are normally attributed to Mie[13], who discovered them independently some years later.

Mie theory predicts the precise form of the electromagnetic field which results from the scattering of a linearly polarised plane wave by a spherical particle of arbitrary size. The theory (see for example Van de Hulst[14] or Kerker[15]) is based on a solution, subject to the appropriate boundary conditions, of a scalar form of the vector wave equation arising from Maxwell's electromagnetic theory. The origin of the co-ordinate system is taken to be the centre of the particle. The Mie solution enables an expression to be written which describes the form of the scattered wave in terms of the amplitude functions $S_1(\theta)$, $S_2(\theta)$ arising from the components of polarisation of the incident wave perpendicular and parallel respectively to the scattering plane:

$$S_1(\theta) = \sum_{n=1}^{\infty} \frac{2n+1}{n(n+1)} \left\{ a_n \frac{1}{\sin\theta} P_n^1(\cos\theta) + b_n \frac{d}{d\theta}\left(P_n^1(\cos\theta)\right)\right\} \qquad (1)$$

$$S_2(\theta) = \sum_{n=1}^{\infty} \frac{2n+1}{n(n+1)} \left\{ a_n \frac{d}{d\theta} P_n^1(\cos\theta) + b_n \frac{1}{\sin\theta}\left(P_n^1(\cos\theta)\right)\right\} . \qquad (2)$$

The scattering plane is defined as the plane containing the incident and scattered wave vectors, and the scattering angle θ is the angle shown in Fig 1. The quantities a_n and b_n are the Mie coefficients and the $P_n^1(\cos\theta)$ are associated Legendre polynomials. The Mie coefficients are complex quantities which depend on the particle size, refractive index and the wavelength of the incident light.

The scattered fields E_1 and E_2, perpendicular and parallel respectively to the plane of scattering, are given at a point distant r from the origin in terms of the incident fields $E_1^{(0)}$ and $E_2^{(0)}$ by:

$$E_1 = S_1(\theta) \exp(ikz - ikr) E_1^{(0)} / ikr \qquad (3)$$

$$E_2 = S_2(\theta) \exp(ikz - ikr) E_2^{(0)} / ikr \ . \qquad (4)$$

Here z is the direction of propagation of the incident plane wave and $k = 2\pi/\lambda$, where λ is the wavelength of the light. The quantity actually measured in any light scattering experiment is the intensity; for perpendicular polarisation

$$I_1(\theta) = |E_1|^2 = i_1(\theta) I_0 / k^2 r^2$$

where

$$i_1(\theta) = |S_1(\theta)|^2 \qquad (5)$$

and for parallel polarisation

$$I_2(\theta) = |E_2|^2 = i_2(\theta) I_0 / k^2 r^2$$

where

$$i_2(\theta) = |S_2(\theta)|^2 \ . \qquad (6)$$

For naturally polarised light

$$I(\theta) = (i_1(\theta) + i_2(\theta)) I_0 / 2k^2 r^2 \qquad (7)$$

I_0 is the intensity of the incident wave.

At this point we introduce the concepts of scattering cross-section and efficiency factor. Imagine a plane wave incident from infinity on a spherical particle. The energy scattered in all directions is equal to the intensity of light from the undisturbed wave which would have fallen on some area C_{sca}; similarly the energy absorbed by the particle is equal to the intensity of the undisturbed incident wave which would have fallen on some area C_{abs}. Finally let the total energy removed from the incident wave be equal to the energy of the undisturbed beam over some area C_{ext}; then the law of conservation of energy requires that the following relationship is true:

$$C_{ext} = C_{sca} + C_{abs} \ . \qquad (8)$$

The quantities C_{ext}, C_{sca} and C_{abs} have dimensions of area and are called the extinction, scattering and absorption cross-sections respectively. These

quantities may be divided by the cross-sectional area of the particle, πa^2, where a is the particle radius, to provide the dimensionless quantities Q_{ext}, Q_{sca} and Q_{abs}, known as the extinction, scattering and absorption efficiencies respectively.

The magnitude of the extinction efficiency can be determined from the amplitude functions, by setting the scattering angle to zero. In this case

$$S_1(0) = S_2(0) = S(0) = \frac{1}{2}\sum_{n=1}^{\infty}(2n+1)(a_n + b_n) \quad .$$

It can be shown that[14]

$$Q_{ext} = (4/\alpha^2)\mathrm{Re}\{S(0)\} \quad , \tag{9}$$

or

$$Q_{ext} = (2/\alpha^2)\sum_{n=1}^{\infty}(2n+1)\mathrm{Re}\{a_n + b_n\} \quad . \tag{10}$$

$\alpha = 2\pi a/\lambda$ is the particle size parameter. Note that the extinction efficiency is independent of the direction of polarisation of the incident wave. For a non-absorbing dielectric sphere, with an entirely real refractive index, $Q_{abs} = 0$ and the scattering efficiency Q_{sca} is equal to the extinction efficiency Q_{ext}. It will be shown that this is effectively the case for particles of interest to this study.

The forms of the intensity functions and the efficiency factors are extremely complex and require the facilities of a large, fast digital computer for their evaluation. However, tables exist for certain combinations of size, refractive index, wavelength and incident polarisation direction. This Report makes use of tables of $Q_{sca}(\alpha)$, due to Penndorf[16], calculated for spherical particles with a purely real refractive index equal to 1.486. It will be shown that this value corresponds closely to the actual value for the oil used in the experiments. A plot of this curve is shown in Fig 2, together with a similar plot for a refractive index of 1.44; this shows the effect of a small change in refractive index on the form of the curve. The intensity functions $I_1(\theta)$, $I_2(\theta)$ and $I_1(\theta) + I_2(\theta)$ shown in Figs 3-6 were derived from a computer program made available by Dave[17] and represent typical functions for a given particle
055 size and refractive index m for a wavelength λ. If, as is normally

the case, the experiment measures the composite scattering function arising from a collection of particles with differing radii then the finer detail in the curves for a mono-dispersion is lost. Under these circumstances a practical unambiguous method of determining the particle size distribution from the experimental data is not known.

2.2 Theory of the angular scattering experiment

One method of overcoming the interpretation problem encountered above was proposed by Sloan[18] who showed that, if the curve $\log I(\theta)\theta^2$ is plotted against the logarithm of scattering angle θ, the position of the first maximum, θ_{max}, is inversely proportional to the mean of some linear characteristic dimension of the particle. The characteristic dimension, in the case of a spherical scattering particle, is the radius a and the expression which relates it to the value of θ_{max} is

$$a\theta_{max} \doteq 9.2 \text{ micron degrees} . \qquad (11)$$

The constant of porportionality (9.2 μm degrees) remains approximately valid over the range of size from 0.2 to 100 microns. Sloan also found that, to a first approximation, the value of θ_{max} for a particular size was independent of the refractive index of the particle. Mie's theory predicts a departure[19] from equation (11) as the size falls below 10 microns which depends on the refractive index. A graph showing the relationship between the exact and approximate values[20] is shown in Fig 7.

2.3 Theory of the extinction experiment

Measurement of the attenuation of a collimated light beam at different wavelengths passing through a suspension of droplets yields information about the particle size[14]. The variation of intensity of a beam of light passing through a cloud of uniformly distributed droplets is proportional to its intensity f so that the extinction occurring in the distance Δz in the direction of propagation is:

$$\Delta f = -\tau f \Delta z . \qquad (12)$$

The constant of proportionality τ is the extinction coefficient. Equation (12) can be integrated to give

$$f/f_0 = \exp(-\tau z) \qquad (13)$$

where f_0 is the intensity of the light at the point from which z is measured. This equation is the Bouger or Lambert-Beer transmittance law. τ can be expressed in terms of the extinction efficiency (Q_{ext}) and the number of particles per unit volume N :

$$\tau = N\pi a^2 Q_{ext} \quad . \tag{14}$$

If the suspension of droplets comprises a size distribution characterised by the function $p(a)$, so that $p(a)\delta a$ is the number of particles per unit volume with radii in the range a to $a + \delta a$, then equation (14) becomes:

$$\tau = \pi \int_0^\infty a^2 p(a) Q_{ext} da \quad . \tag{15}$$

The quantity f/f_0 can be measured at a number of different wavelengths. Thus if the form of the function $p(a)$ is known or if the suspension is assumed to be mono-disperse, the curve of $\log_e f_0/f$ plotted against the wavenumber ν , defined by $\nu = \pi/\lambda$, can be fitted to a similar, calculated plot of $Q_{ext}(\alpha)$; we recall that $\alpha = 2\pi a/\lambda$. Comparison of the abscissae yields the particle size, which in the case of a mono-dispersion is the common diameter. In the case of a particle size distribution[21] it is the Sauter mean diameter, defined as the ratio of the third to the second moments of the size distribution.

3 EXPERIMENTS

The interpretation of the results obtained from light scattering experiments, described in this section, requires a knowledge of the complex refractive index of the oil.

3.1 Measurement of the refractive index of the oil

The complex refractive index m is conventionally written in the form:

$$m = n_r - in_i \quad . \tag{16}$$

The real part n_r is related to the velocity of propagation of an electromagnetic wave through the medium and is the part used for the calculation of, for example, the angles of refraction. The imaginary part n_i describes the attenuation of the wave as it passes through the medium (*ie* the process of absorption). The
055 equation for the electric field component of an electromagnetic wave propagating

in the z direction with an angular frequency ω can be written in terms of the refractive index m :

$$E = E_0 \exp\{- i\omega(t + mz)\} \tag{17}$$

E_0 is the amplitude of the electric field at the point from which z is measured. The intensity $|E|^2$ at any point in the medium is given by the formula

$$I = I_0 \exp(- Kz) \tag{18}$$

where I_0 is the quantity $|E_0|^2$ and K is the absorption coefficient:

$$K = 4\pi n_i/\lambda_0 \ , \tag{19}$$

λ_0 is the wavelength of the radiation *in vacuo*.

Measurement of the quantity I/I_0 at a given wavelength λ and over a distance z yields the imaginary part of the refractive index n_i . The schematic layout of such an experiment is shown in Fig 8. It is important to restrict the power density in the test cell, otherwise distortion of the laser beam may occur through absorption of energy and consequent heating of the oil. The distortion will arise from the local change in the real part of the refractive index n_r . Note that this quantity, for liquids, is very sensitive to temperature; for example $\Delta n_r/\Delta T$ for water is $\doteq 10^{-4}$ per degree centrigrade[22].

The value of the real part of the refractive index was determined from an experiment with a hollow prism in a simple spectrometer. The prism, which contains the oil, was constructed from microscope slides; the geometry is shown in Fig 9. Measurement of the angles of incidence $\hat{\alpha}$ and refraction $\hat{\beta}$ would yield, via Snell's law, the quantity n_r if direct measurement of the angle $\hat{\beta}$ were practicable. Using the optical arrangement shown in Fig 10 it is possible to measure the angles $2\hat{\alpha}$ and $\hat{\rho}$ and, with an accurate knowledge of the internal angle $\hat{B}$, it is possible to evaluate the refractive index from the following relationships:

$$n_r \cos \hat{\beta} = (\sin \hat{\delta} + \cos \hat{B} \sin \hat{\alpha})/\sin \hat{B} \tag{20}$$

$$\sin \hat{\beta} = (\sin \hat{\alpha})/n_r \tag{21}$$

$$\hat{\delta} = \hat{B} - \hat{\alpha} + \hat{\rho} - \pi \ . \tag{22}$$

The internal angle $\hat{B}$ was first determined by measuring the angles $2\hat{\alpha}$ and $\hat{\rho}$ for a liquid with a known refractive index[22] (distilled water) and then using relationships (20) to (22) for this value of n_r.

In practice, because the oil and water are immiscible, both experiments could be carried out together and a set of angles $\hat{\rho}$ obtained for a constant angle of incidence $\hat{\alpha}$ and a selection of wavelengths (577, 546 and 436 nm), for both the oil and the water.

Although subsequent light scattering experiments employed lasers exclusively, a mercury vapour source was used for these measurements, mainly to avoid the diffraction effects associated with highly coherent light.

The results for the real part of the refractive index were extended to the required laser wavelengths 632.8, 514.5, 488.0 and 457 nm by use of the Cauchy dispersion relationship[23]:

$$n_r = A + \frac{B}{\lambda^2} + \ldots\ldots .$$

3.2 Angular intensity measurements

The Mie theory, outlined above, gives the form of the intensity functions $i_1(\theta)$, $i_2(\theta)$ which would arise from scattering by a single particle. The determination of these quantities would require the selection and positioning of the particle while measurements were carried out. One possible method of achieving this would be an adaptation of the Millikan[24] oil drop experiment, although this would require a complex position-control system and an optical enclosure, which could give rise to parasitic radiation.

An alternative technique is described in Ref 25 which employs a high speed rotating mirror to change the scattering angle θ and accumulates data from the light scattered by particles which pass slowly through the sample volume. This system works over a limited range of θ and also requires the integration of the scattered light from many successive particle transits to provide adequate signals for analysis.

The method adopted here avoids the use of an enclosure and therefore the problems associated with parasitic radiation, by analysing, with a collimated detection system, the light scattered by a fine stream of particles, illuminated by a focused laser beam. A schematic diagram of the experiment is shown in Fig 11. Note that in a typical laser anemometry application the seeding particles

are introduced into the gas in a similar manner, and also that during the course of an anemometry experiment the detector is exposed to the scattered light field arising from the whole particle size distribution.

The basic optical system consists of three parts, an illumination system, a detector arm that can move in the scattering plane over a range of θ and a static reference arm. The first part uses the radiation from an argon-ion laser (Spectra-Physics Model 165), operated in the constant power output mode at approximately 200 mW. The output beam is expanded by a lens L_1 and focused to a waist by lens L_2. The diameter of the waist, approximately 10 microns, was calculated from measured input beam characteristics using the expressions derived by Kogelnik and Li[26]. Measurements of the diameter of the laser beam as it expanded away from the waist confirmed this value. Plots of the beam profile and the axial power distribution are shown in Fig 12. The output of the laser is vertically polarised by virtue of the orientation of the Brewster windows within the cavity. Hence, in order to measure $I_2(\theta)$ with the same experimental arrangement a rotation of 90 degrees of the direction of polarisation direction is required. This was achieved using a half wave plate P_1.

The second part of the optical system, the movable detector arm, consisted of a long collimating tube which could describe an arc in the horizontal scattering plane, centred on the intersection of the axes of the particle jet and the illuminating laser beam. The range of θ covered was from 10 to 160 degrees. It was not possible to reduce the lower limit because the rapidly expanding laser beam beyond the sample volume interfered with the scattered light signal. The value of the scattering angle was determined from a large, graduated rotating table which formed part of the mechanical arrangement.

The collimating tube defined a collection angle of approximately 6.7 mrad ($\triangleq$0.38 degrees) by means of two 1mm diameter apertures separated by a light tight tube approximately 300 mm long. Attached to the rear of this tube was a photon counting photomultiplier tube, type ITT FW 130, fitted with a narrow band filter, matched to the laser wavelength (488 nm), and an imaging lens which focused the rear aperture of the collimating tube on to the photo-cathode. The photo-multiplier tube is housed in a light tight case which also contains discriminator and pulse shaping electronics. The output from the detector consists of a train of identical pulses whose mean repetition rate is proportional to the intensity of the light incident on the photo-cathode.

The third part of the optical system is the monitor arm; this consists of a similar, but fixed, arrangement to the moving arm. It is positioned at a

scattering angle of approximately 60 degrees, but on the opposite side of the illuminating laser beam to the moving arm. Together with readings of the laser power meter, it provides the means of correcting for the fluctuations in the number of the particles passing through the scattering volume.

For convenience the output pulses from the photomultipliers were counted by the Malvern digital autocorrelator, type K7023. This had the advantage that it simplified the experimental procedure. For each angle, the total number of photon-detections could be counted over a preset period and automatically recorded on paper tape for subsequent analysis.

The particle generation and filtering arrangement is shown in Fig 13. It consists of a commercial oil-mist generator (Norgren micro-fog), intended for use in lubricating systems, and an optional 5 litre settling chamber. This could be used to remove large particles, formed by agglomeration, and to smooth out fluctuations in the number of particles passing through the sample volume. The mean rate at which the particles were produced was controlled by adjusting the drip-rate and hence the volume of the oil supplied to the atomising venturi section.

The seeds were delivered to the scattering region at a pressure slightly above atmospheric and launched into the atmosphere through a narrow glass tube, approximately 1 mm in diameter, as shown in Fig 11. In order to avoid contamination of the optics and to prevent the accumulation of oil droplets in the laboratory, the particles were drawn away from the scattering region by an exhauster; this also provided a moving sheath of air around the scattering region which limited the ingress of dust particles from the laboratory.

The experiment was carried out by recording the total number of photon-detections (counts) from the detectors, in some convenient time (10 seconds) at each scattering angle θ . This was repeated a number of times, at each angle, to enable the elimination of abnormally high counts to be carried out; these anomalies could arise from example when a large agglomerated particle passed through the scattering volume.

A complete set of experiments was performed over the entire range of scattering angles θ (10-160 degrees) in 5 degree steps and a comparative set of experiments was carried out for the cases where the particles were absent and the laser beam switched off. This permitted corrections to be made to the scattering results for the effect of background radiation.

3.3 Extinction measurements

This experiment was carried out in an attempt to verify the results for particle size obtained from the angular scattering measurements described above. However, the interpretation of the measurement depends on the assumption that the micro-fog generator produces particles with a narrow size distribution (*ie* a near-monodispersion). In addition the technique requires the experimentally derived points ($\log_e f_0/f$ plotted against ν) to be matched to the curve $Q_{ext}(\alpha)$. However, for the range of α over which the experiment can easily be carried out this method is subject to large errors. In addition there is the conflicting requirement that the experimental range of wavelengths and hence the range of values of α should be limited, or the dispersion of the oil (change in refractive index with wavelength) will cause a significant change in the curve $Q_{ext}(\alpha)$; see Fig 1.

The extinction experiment is designed to measure the extinction coefficient τ of a suspension of oil droplets (produced by the oil-mist generator) at a number of different wavelengths and simultaneously to measure the relative number of particles present in the sample volume. This was carried out with the arrangement shown in Fig 14.

Two laser beams, at different wavelengths, pass coaxially through the droplet suspension; the attenuation of one of the beams is used to monitor the relative number of droplets per unit volume N, whilst the second beam gave the relative attenuation at a different wavelength for the same droplet density. The optical system thus has three functions: to provide, simultaneously, a pair of coaxial collimated beams at different wavelengths; to provide an enclosure for the droplet suspension; and to provide a receiving system which accepts only the unscattered light.

The first function is fulfilled by combining the outputs of an argon-ion laser and a helium-neon laser at the interface of a beamsplitter B as shown in Fig 14. The resulting coaxial beam is expanded and collimated by the arrangement L_1, L_2. The diameter of the collimated beam was approximately 10 mm. The power of each laser beam was monitored by detectors D_1 and D_2 via the dispersing prism P_1. The wavelengths available for use were 632.8 from the He-Ne laser and 457, 488 and 514.5 nm from the argon-ion laser.

The second function of the optical system, the enclosure, was provided by a 1.5m tube made from resin-bonded paper. It was 150 mm in diameter and fitted with perspex ends, holding removable glass windows. Oil mist from the generator,

with or without the settling chamber in circuit, was introduced into the tube at a tangent to the wall, in order to provide a homogeneous distribution of droplets within the sample volume. The mist was exhausted from the opposite end of the tube and expelled from the laboratory to prevent the accumulation of droplets in the transmission paths external to the test cell. To provide an overall attenuation of the transmitted beam of 80%, as recommended by Hodkinson[27], it was necessary to reflect the beams back through the optical cell, providing a total path length of $z = 3.0$ m.

The coaxial beams emerging from the cell were split into two parts by the Amici prism P_2 and passed directly to the receiving optics, which consisted of a focusing lens, aperture and detector; these components were selected to fulfil the third function, of angular separation of the transmitted and scattered light. Hodkinson[27] claims that if the angle subtended by an aperture at its associated lens is less than one-tenth of the angle of the first minimum of the Fraunhofer diffraction pattern resulting from the largest particle in the scattering volume, then the angular resolution of the receiving system is adequate. The combinations of lens and aperture $L_3 - A_1$ and $L_4 - A_2$ used in this study gave sufficient resolution with this criterion for particles up to 7 microns in diameter (for a wavelength of 500 nm). Note that providing the criterion is met the beams do not have to be accurately collimated.

The detectors $D_1 - D_4$ are large area silicon photodiodes, type BPY 13A; operated in the reverse bias mode, these detectors have a linear response to light intensity over the range of interest.

The first part of the experiment consists of selecting the appropriate wavelength of the argon-ion laser, aligning the optics and measuring the currents through the photo-detectors; this corresponds, with the cell empty, to the measurement of the incident intensity f_0 for both wavelengths. The cell is then gradually filled with oil droplets until equilibrium is reached, when the number of particles per unit volume is constant; at this point the transmitted intensities f are measured for both wavelengths, simultaneously; in addition a note is made of the monitor diode currents.

The experiment is repeated for different combinations of wavelength and filtering (of the particles). The data reduction consists of subtracting the dark currents from the detector values, standardising the value of f against fluctuations in laser power and eliminating the particle number density by deriving a relative extinction coefficient for each wavelength, compared to the

He-Ne extinction. The points corresponding to the relative value of $\log_e f_0/f$ plotted against wave number (ν) are then fitted to the plot of $Q_{ext}(\alpha)$ obtained from Penndorf's data for monodispersions with a refractive index of 1.486.

4 RESULTS AND DISCUSSION

4.1 Refractive index measurements

The absorption of the laser beam passing through 78 mm of the OM-11 light mineral oil, at approximately 22°C, was found to be approximately 2.5% at a wavelength of 488 nm. The value of the absorption coefficient, defined in equation (19), was therefore 0.32 m^{-1}, which leads to a value of 1.26×10^{-8} for the imaginary part of the refractive index, n_i .

The value of the real part of the refractive index, n_r , was measured at several wavelengths and calculated for the remaining laser wavelengths. The results are summarised in Table 1.

Table 1

Real part of refractive index n_r	1.475*	1.477	1.479	1.481*	1.483*	1.486*	1.488
Wavelength nm	632.8	577	546	514.5	488.0	457	436

* Indicates estimated value (using Cauchy relationship)

It can be seen from the table that the value of the refractive index changes by less than 1% over the wavelength range 436-632.8 nm, so that the calculated curve for $Q_{ext}(\alpha)$ for the value 1.486 is adequate for the interpretation of the results from the extinction experiment, since other errors, for example from curve fitting, are more significant.

4.2 Angular scattering intensity measurements

Figs 15 to 16 show the curves $I_1(\theta)$, $I_2(\theta)$ obtained from the experiment described above. As can be seen the curves show none of the detailed structure predicted by the Mie theory. This suggests that the particle population is a polydispersion, although the degree of dispersity required to produce such smooth curves is not known. Some insight may be gained by inspection of the curves drawn in Figs 3 to 6, which show that small variations in the particle size parameter α produce large changes in the structure of the curves.

It can be seen from the measured distribution that a laser anemometer collecting light in the near back-scatter direction $\theta \triangleq 160$ degrees receives far less signal than in the corresponding forward scatter direction. The minimum intensity of the scattered light from the particles used at RAE appears to lie at around 120 degrees.

The angular dependence of the scattered light intensity for unfiltered particles (Fig 16) shows relatively greater forward scattering than in the case of the filtered particles (Fig 15). This is consistent with the presence of larger particles in the scattering volume.

The derived Sloan-type plots for the results obtained with the settling chamber are drawn in Fig 17 for the two polarisation states. The curves have clear first maxima at angles of 38 degrees and 44.6 degrees which yield from equation (11) values of 0.48 and 0.41 microns for the mean diameter estimates. On the assumption that the particles are a true monodispersion, the Mie theory based correction for the refractive index and particle size (Fig 7) would give corresponding diameters of 0.51 and 0.44 microns. These values are consistent with experience gained in the laser anemometry experiments in rapidly accelerating flows referred to in the introduction, and also agree with an independent investigation of particle size carried out by Gregory[20].

4.3 Extinction measurements

Fig 18 shows the limited number of points, derived from measurements of the relative extinction, fitted to the curve of $Q_{ext}(\alpha)$. It clearly shows the difficulty encountered in interpreting the measurements; however the correspondence of the abscissae indicates that the particle diameter is approximately 0.71 microns for the filtered particles. Measurements made on the unfiltered particles indicated that they had a rather larger diameter (0.74 microns).

5 CONCLUSIONS

The results of the experiments confirm that the seeding particles used at present for wind-tunnel laser anemometry at RAE are suitable for most applications of interest. The results obtained from the experiments show that the particles are well within the diameter range 0.1 to 1.0 microns, which accords with experience gained in wind-tunnel experiments on strongly accelerating flows. The values around 0.5 micron for the mean diameters obtained from the Sloan plots are more reliable in view of the difficulty of interpreting the other forms of data.

The experiments have also shown that large particles can agglomerate in the seeding system and that these must be filtered out if misleading estimates of velocity in highly accelerating flows are to be avoided. It has also been shown from the shape of the angular intensity distribution of the scattered light that, for anemometry experiments using this type of seeding, scattering angles around 120 degrees should be avoided.

The overall conclusion reached in this study is that the accurate determination of the size of the particles whose diameter is similar to the incident wavelength is very difficult using light scattering techniques. Although more detailed size experiments on the oil droplets are probably not necessary for existing anemometry applications at RAE, an experiment of the Millikan type where measurements can be carried out on a single particle would be very instructive. Methods based on Fraunhofer diffraction at ultra-violet wavelengths could also possibly be developed to yield estimates of the size distribution.

Acknowledgments

I would like to thank the following people for their assistance in the production of this Technical Report: J.B. Abbiss for his advice and criticisms; R. Allan and T. McCord for the calculation of Figs 3 to 6; and T.P. Read for practical assistance with the experiments.

REFERENCES

No.	Author	Title, etc
1	J.B. Abbiss L.F. East C.R. Nash Patricia Parker E.R. Pike W.G. Sawyer	A study of the interaction of a normal shock wave and a turbulent boundary layer using a laser anemometer. RAE Technical Report 75141 (1975)
2	J.B. Abbiss T.W. Chubb A.R.G. Mundell C.J. Oliver E.R. Pike P.R. Sharpe	Laser anemometry in an unseeded supersonic wind tunnel by means of photon-correlation spectroscopy of back-scattered light. J. Phys. D., 5, pp 100-102 (1972)
3	R.G. Boothroyd	Tracer behaviour in laser anemometry for turbulent flow. Optics and Laser Technology, April 1972
4	A.M. Karchmer	Particle trackability considerations for laser Doppler velocimetry. NASA Technical Memorandum X-2628 (1972)
5	K.J. Kirsch M.K. Mazumder	Aerosol size spectrum analysis using relaxation time measurement. Applied Physics Letters, 26, 4 February 1975
6	W.J. Yanta	Measurement of aerosol size distribution with a laser Doppler velocimeter. AIAA Paper 73-705, July 1973
7	H.D. vom Stein H.J. Pfeifer	Investigation of the velocity relaxation of micron sized particles in shock waves using laser radiation. Applied Optics, 11, 2 February 1972
8	B.R. Maxwell R.G. Seasholtz	Velocity lag of solid particles in oscillating gases and in gases passing through normal shock waves. NASA Technical Note D-7490, March 1974
9	J.B. Abbiss T.W. Chubb	Proceedings of the Technical Programme, Electro-Optics International Conference, March 1974 London, Kiver Communications
10	L.F. East	Applications of non-intrusive instrumentation in fluid flow research. AGARD CP-193, May 1976

REFERENCES (continued)

No.	Author	Title, etc
11	Ministry of Supply (Air Division)	Specification No. D.ENG.R.D.2490 (Issue 1) 1953, amended 1955
12	-	Oeuvres Scientifiques de L. Lorenz, translated by H. Valentine. Copenhagen, Librarie Lehemann and Stage (1898)
13	G. Mie	Ann der Physik, 4, 25, pp 377-445 (1908)
14	H.C. Van de Hulst	Light scattering by small particles. New York, Wiley and Sons (1957)
15	M. Kerker	The scattering of light and other electromagnetic radiation. London, Academic Press (1969)
16	R.B. Penndorf	New tables of total Mie scattering coefficients for spherical particles of real refractive indexes. ($1.33 \leqslant n_r \leqslant 1.50$). J. Opt. Soc Amer., 47, 11 November 1957
17	J.V. Dave	Subroutines for computing the parameters of the electromagnetic radiation scattered by a sphere. IBM Scientific Centre, Palo Alto, California. Report No. 320-3237 (1968)
18	C.K. Sloan	Angular dependence light scattering studies of the ageing of precipitates. J. Phys. Chem., 59, pp 834-840 (1955)
19	E.J. Meehan A.E. Gyberg	Particle size determination by low angle scattering: effect of refractive index. Applied Optics, 12, 3, pp 551-554 (1973)
20	D.A. Gregory	Aerosol seeding techniques for laser anemometry in wind-tunnel applications. British Aircraft Corporation Report ST 13928 (1975)
21	P.T. Walters	Optical measurement of water droplets in wet steam flows. Heat and Fluid flow in steam and gas turbine plant. Conference Paper, University of Warwick, 3-5 April, 1973, London Institute of Mech. Eng.

REFERENCES (concluded)

No.	Author	Title, etc
22	G.W.C. Kaye T.H. Labey	Tables of physical and chemical constants. 14th edition, London, Longman (1973)
23	R.S. Longhurst	Geometrical and Physical Optics. 2nd edition, pp 452-3, London, Longman (1967)
24	R. Millikan	Phys. Rev., 32, p 349 (1911)
25	E.R. Pike H.Z. Cummins	Photon correlation spectroscopy and velocimetry. B23. New York, Plenum Press, pp 301-304 (1977)
26	H. Kogelnik T. Li	Applied Optics, 5, 10, pp 1550-1567 (1966)
27	J.K. Hodkinson	The optical measurement of aerosols. London Academic Press (1966)

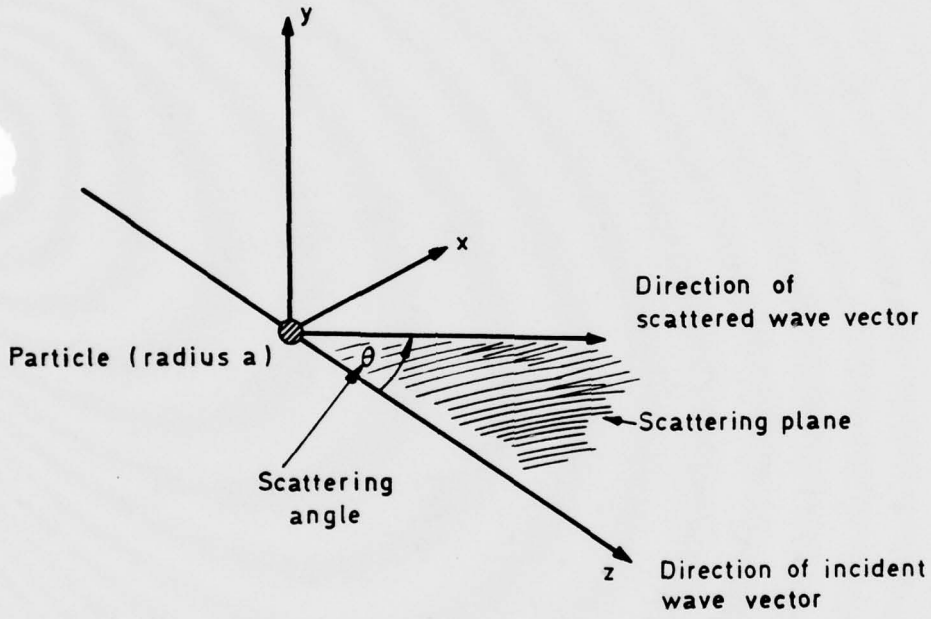

Fig 1 Co-ordinate system

Fig 2

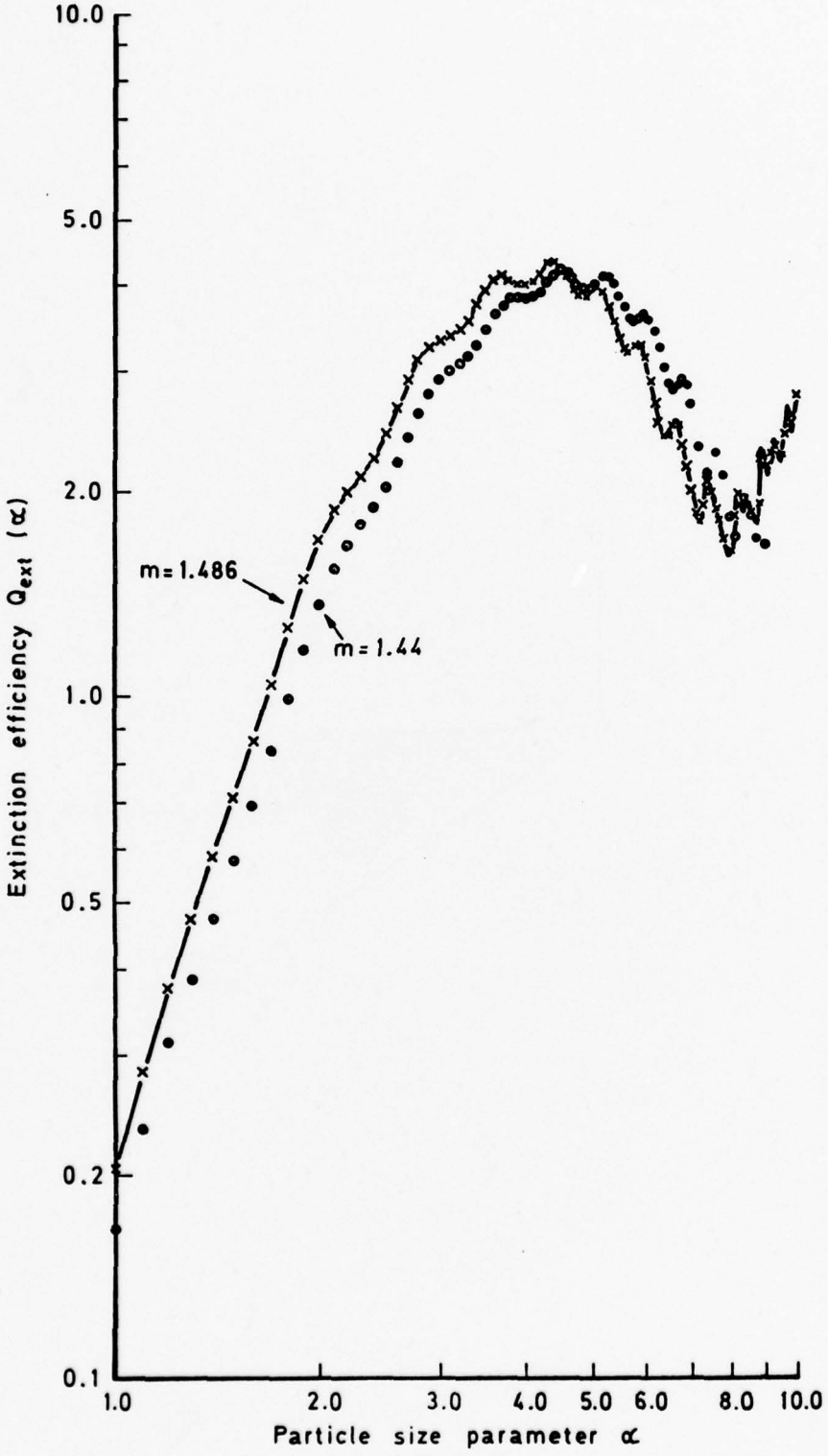

Fig 2 Comparative plots of $Q_{ext}(\alpha)$.
For refractive indices of 1.44 and 1.486

TR 78055

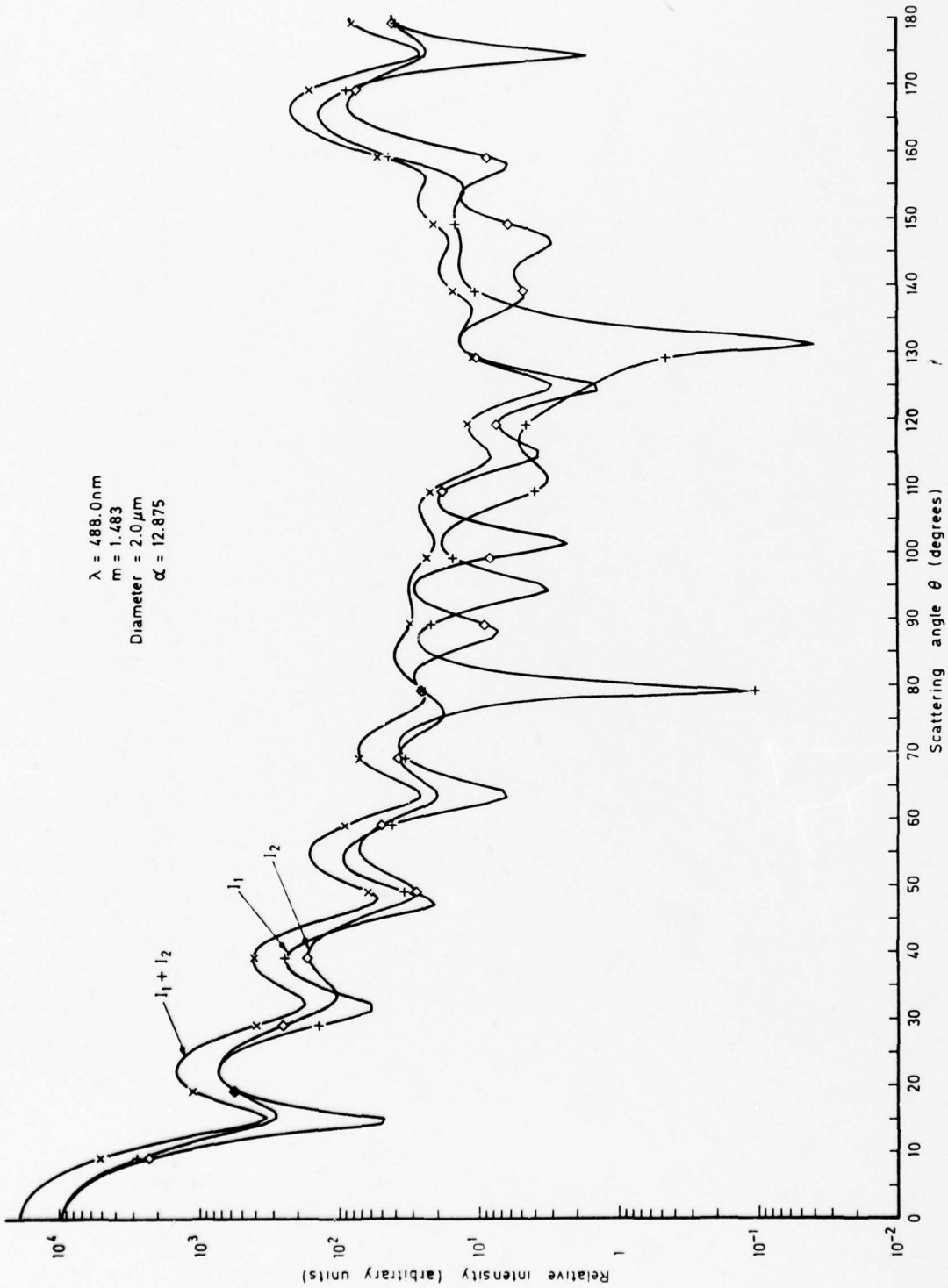
λ = 488.0nm
m = 1.483
Diameter = 2.0μm
α = 12.875
$I_1 + I_2$
I_1
I_2
Relative intensity (arbitrary units)
Scattering angle θ (degrees)
10^4
10^3
10^2
10^1
1
10^{-1}
10^{-2}
0
10
20
30
40
50
60
70
80
90
100
110
120
130
140
150
160
170
180

Fig 3

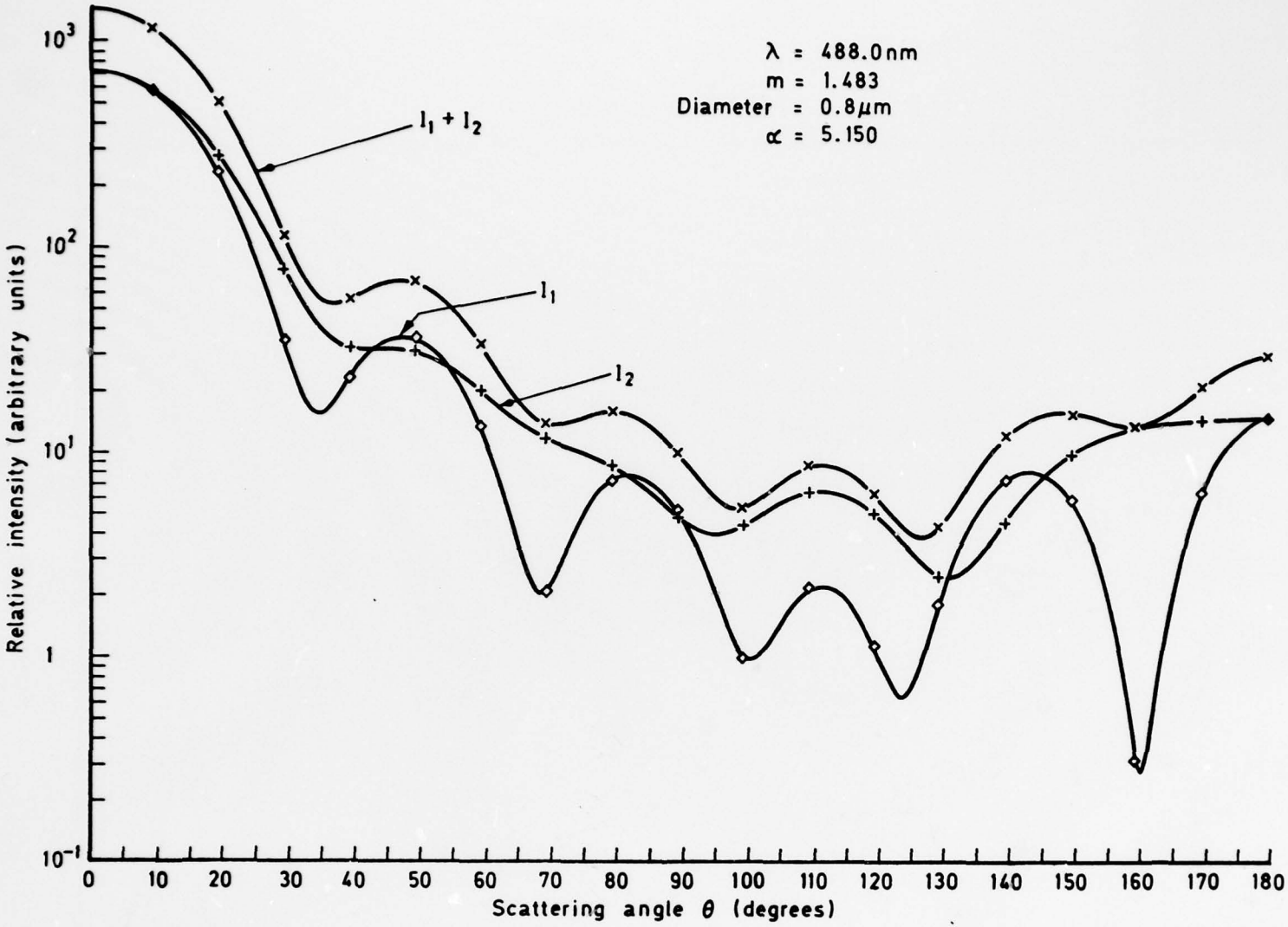
λ = 488.0nm
m = 1.483
Diameter = 0.8μm
α = 5.150
$I_1 + I_2$
I_1
I_2
Relative intensity (arbitrary units)
10^3
10^2
10^1
1
10^{-1}
0 10 20 30 40 50 60 70 80 90 100 110 120 130 140 150 160 170 180
Scattering angle θ (degrees)

Fig 4

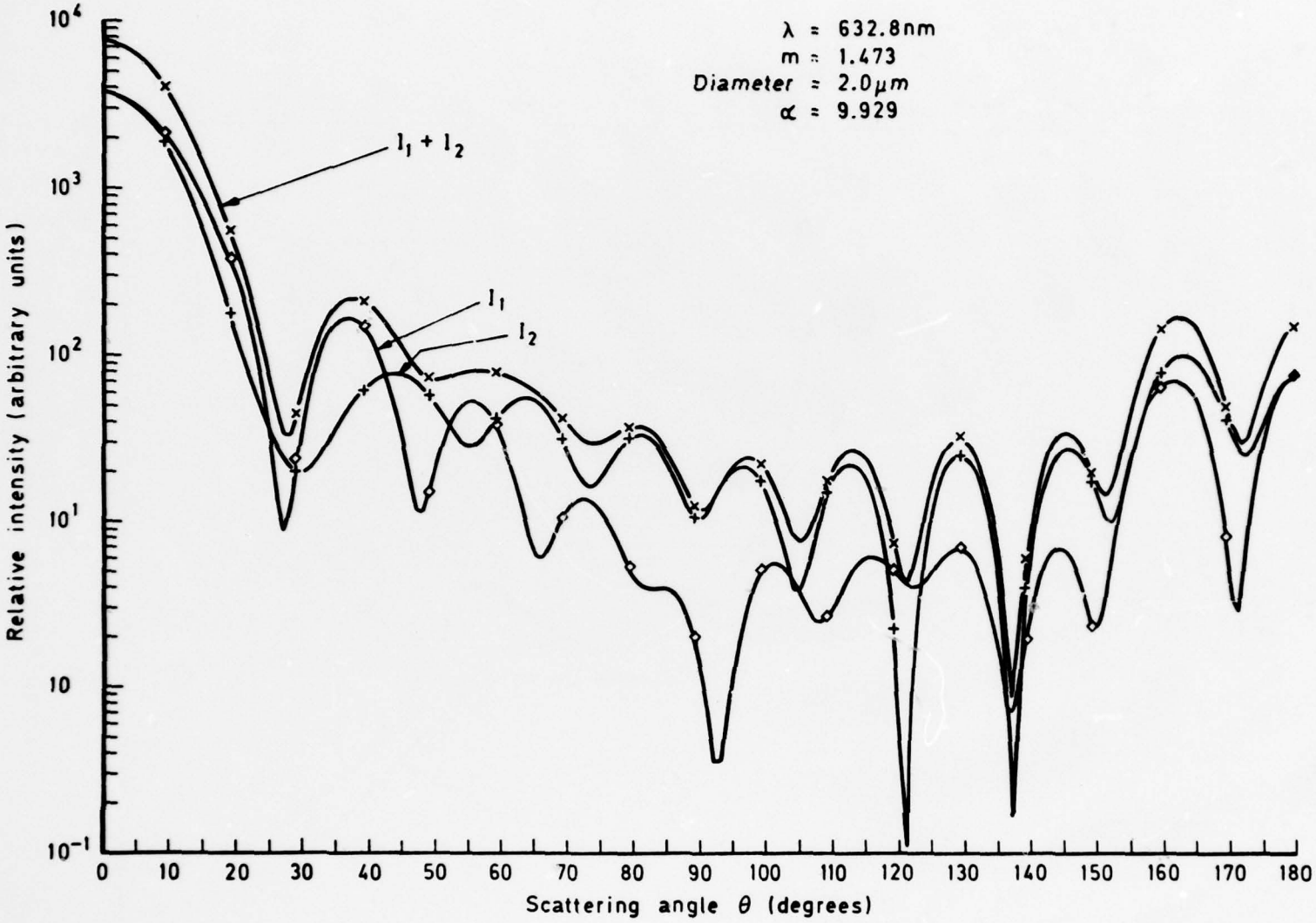
λ = 632.8nm
m = 1.473
Diameter = 2.0μm
α = 9.929
$I_1 + I_2$
I_1
I_2
Relative intensity (arbitrary units)
10^4
10^3
10^2
10^1
10
10^{-1}
0 10 20 30 40 50 60 70 80 90 100 110 120 130 140 150 160 170 180
Scattering angle θ (degrees)

Fig 5

Fig 5

Fig 6

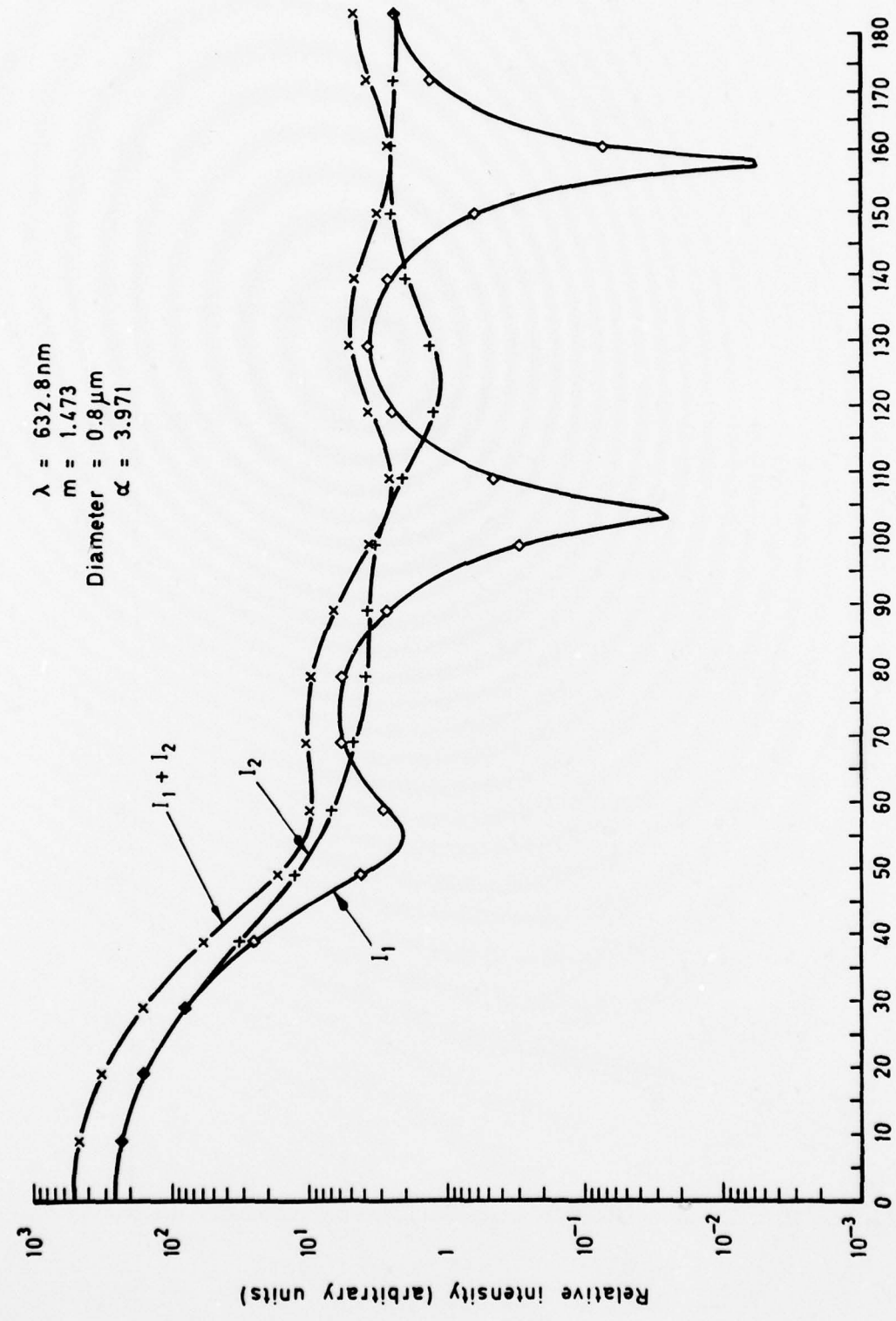

Fig 6

TR 78055

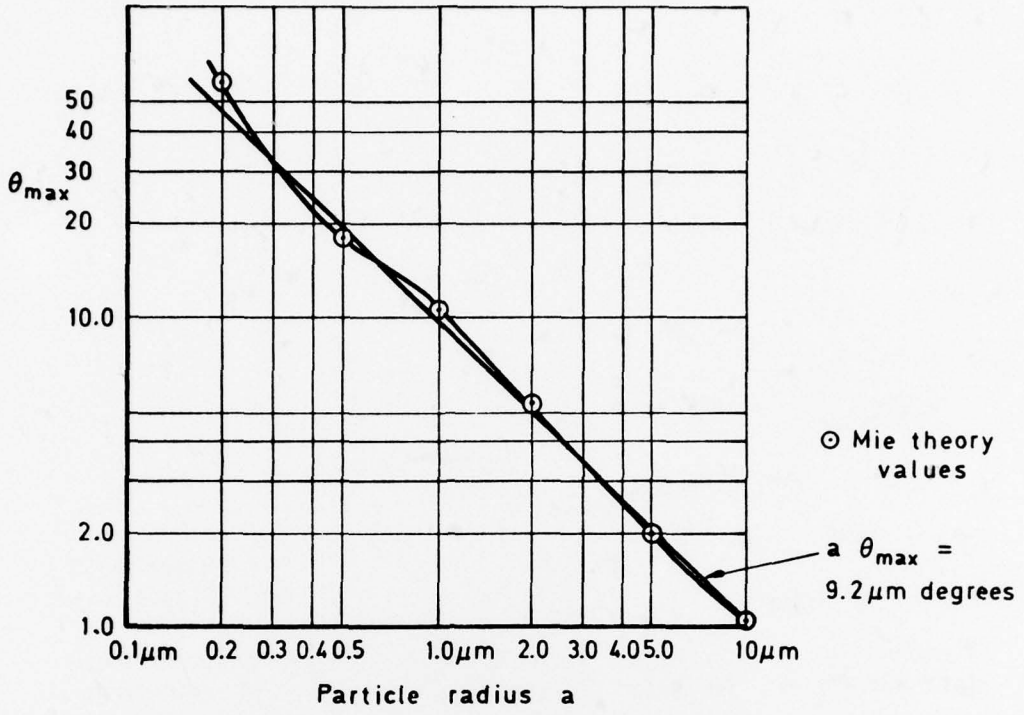

Fig 7 MIE theory correction for Sloan estimates of radius

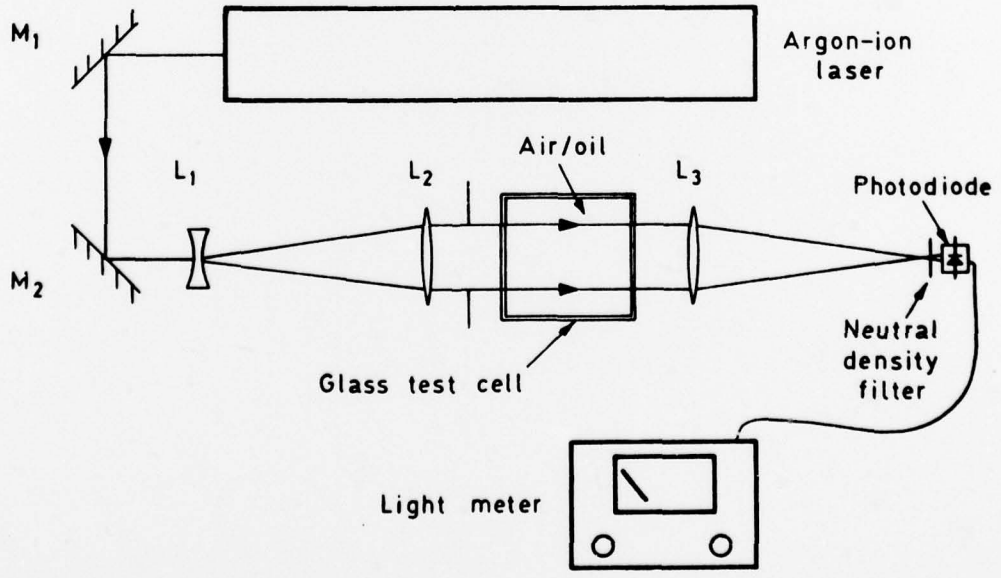

Fig 8 Measurement of the imaginary part of the refractive index (n_i)

Fig 9

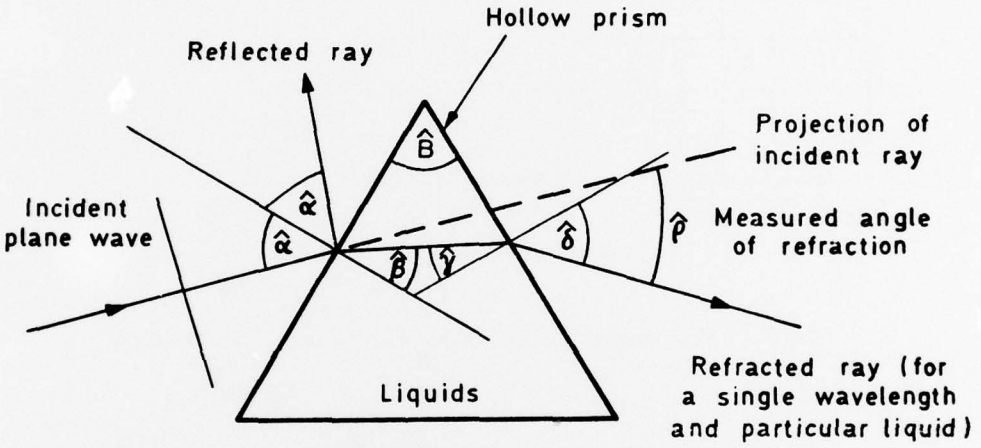

Plan view

Fig 9 Geometry of hollow prism

TR 78055

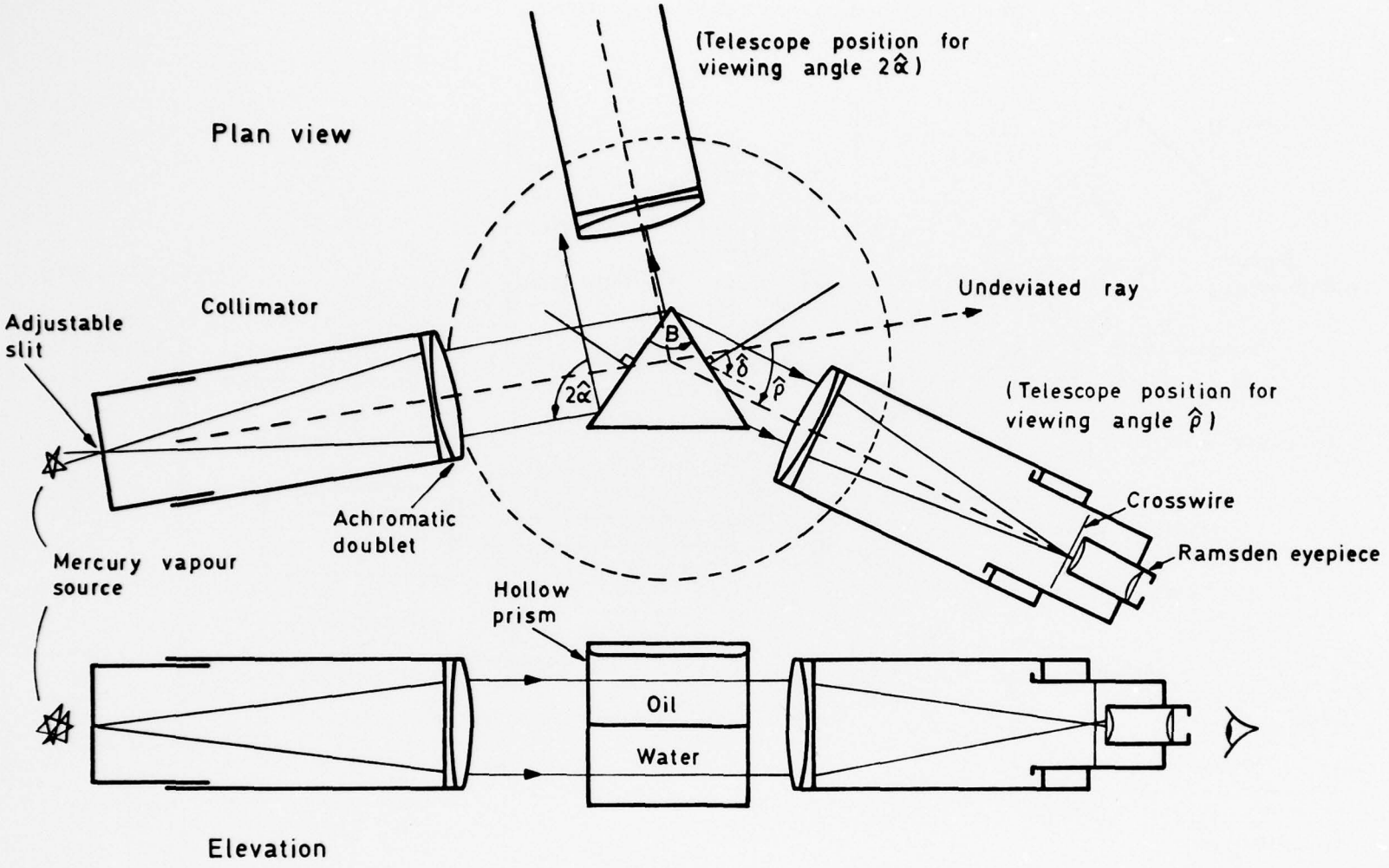

Fig 10 Experimental arrangement for measurement of real part of refractive index (n_r)

Fig 10

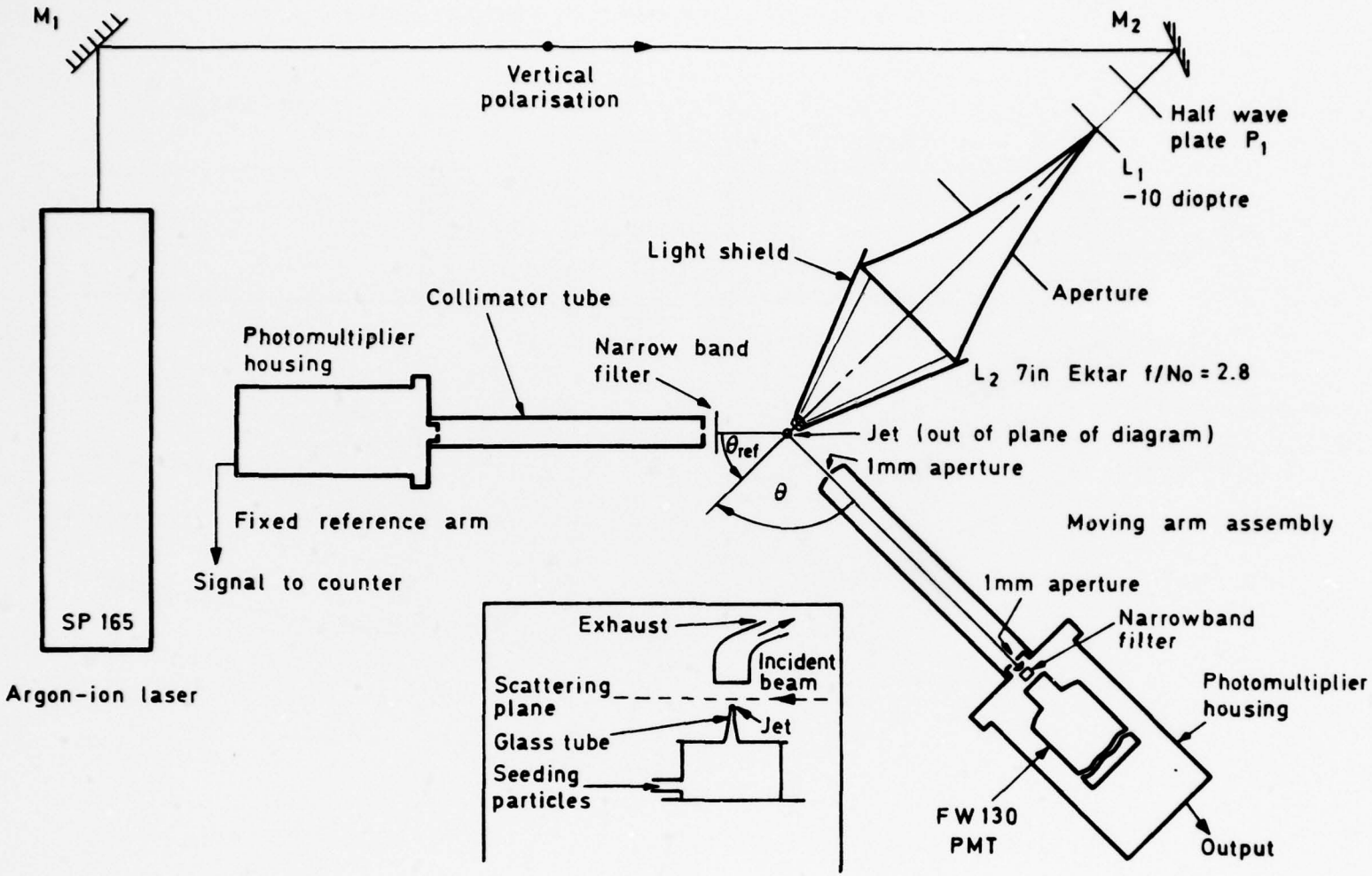

Fig 11 Schematic diagram of angular scattering experiment

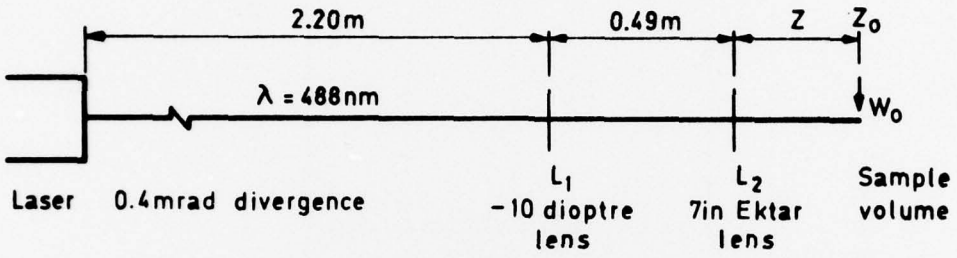

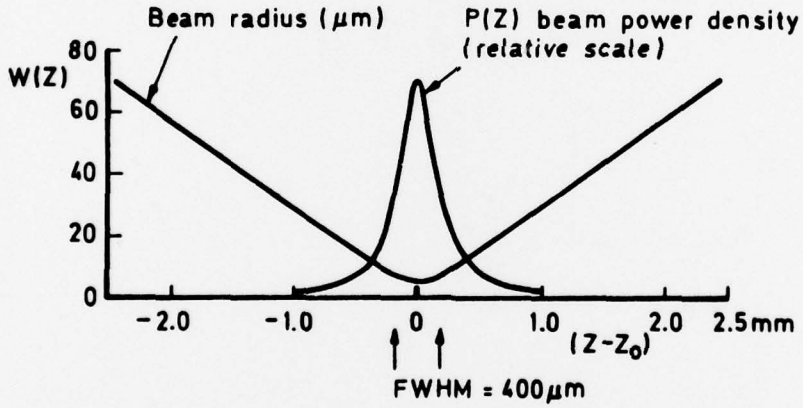

Fig 12 Beam characteristics

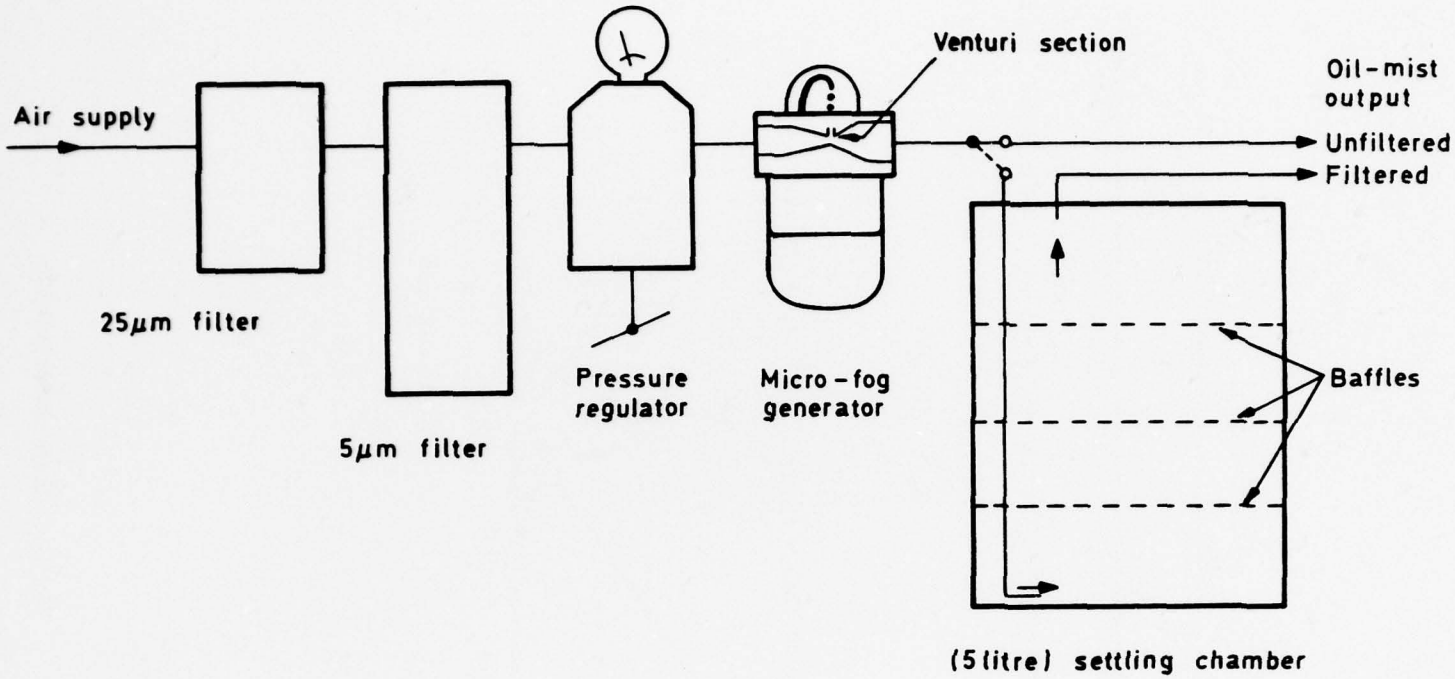

Fig 13 Particle (oil-mist) generator

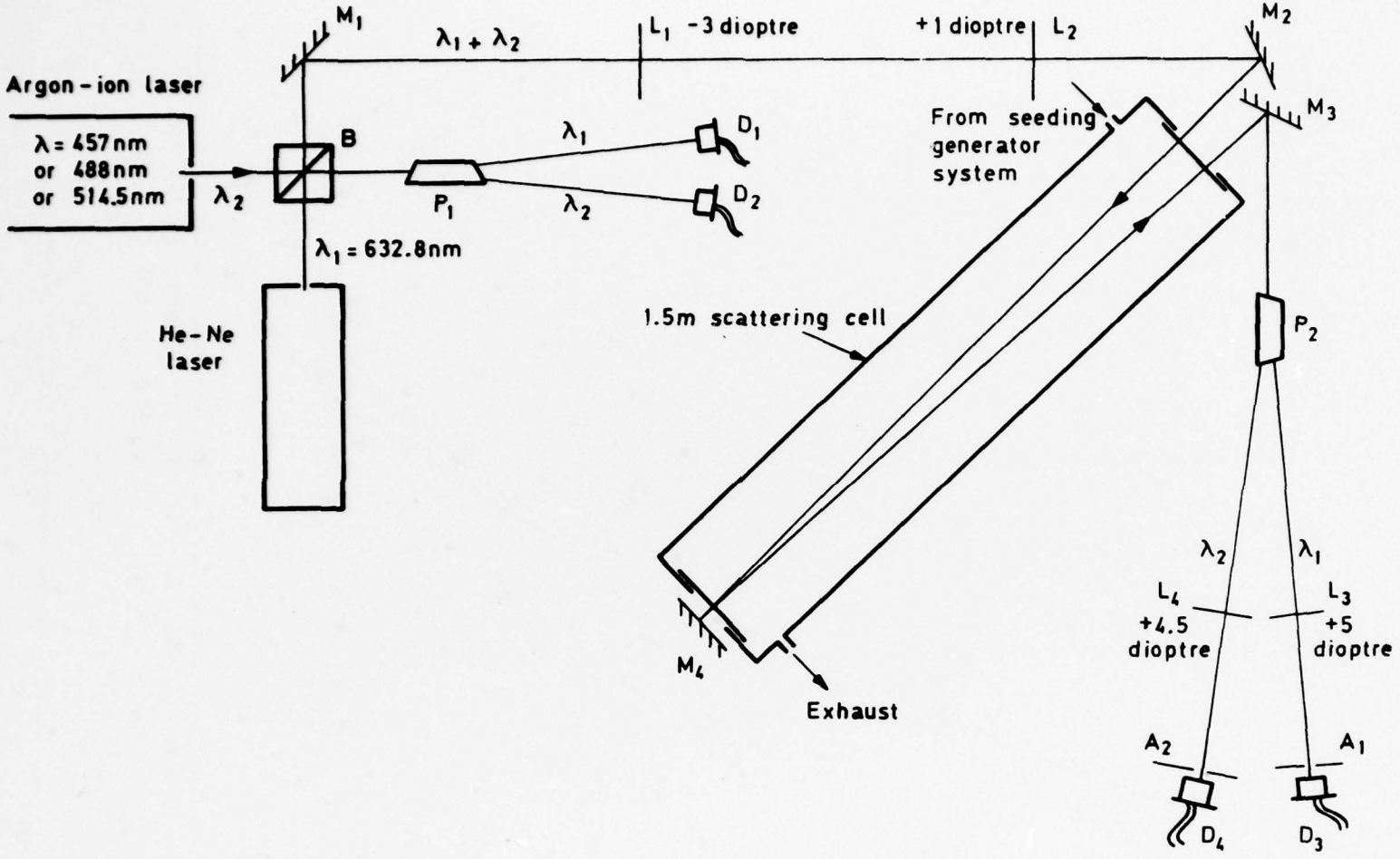

Fig 14 Optical arrangement of extinction experiment

Fig 14

Fig 15

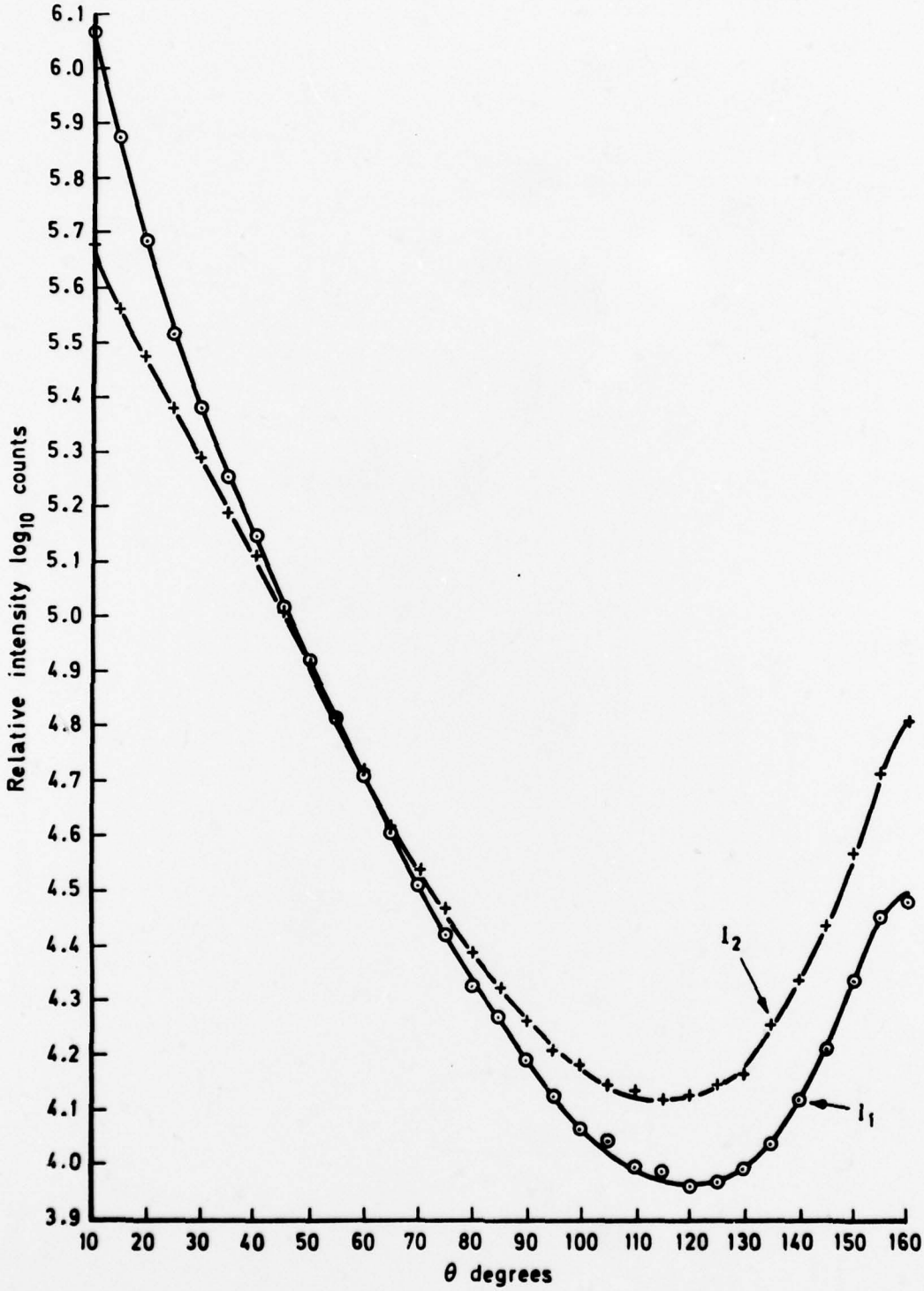

Fig 15 Angular scattering intensity for the filtered particles

TR 78055

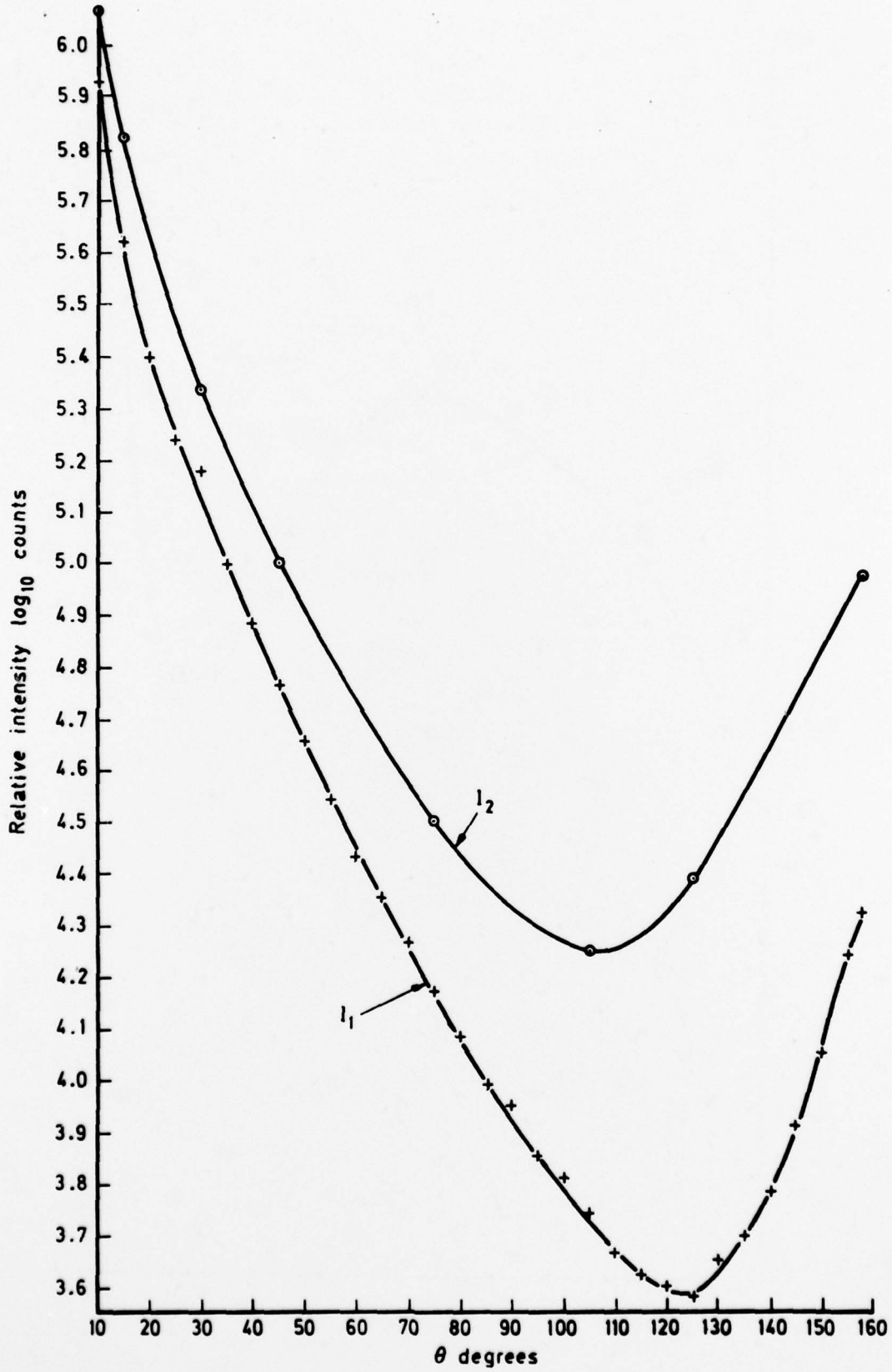

Fig 16 Angular scattering intensity for the unfiltered particles

Fig 17

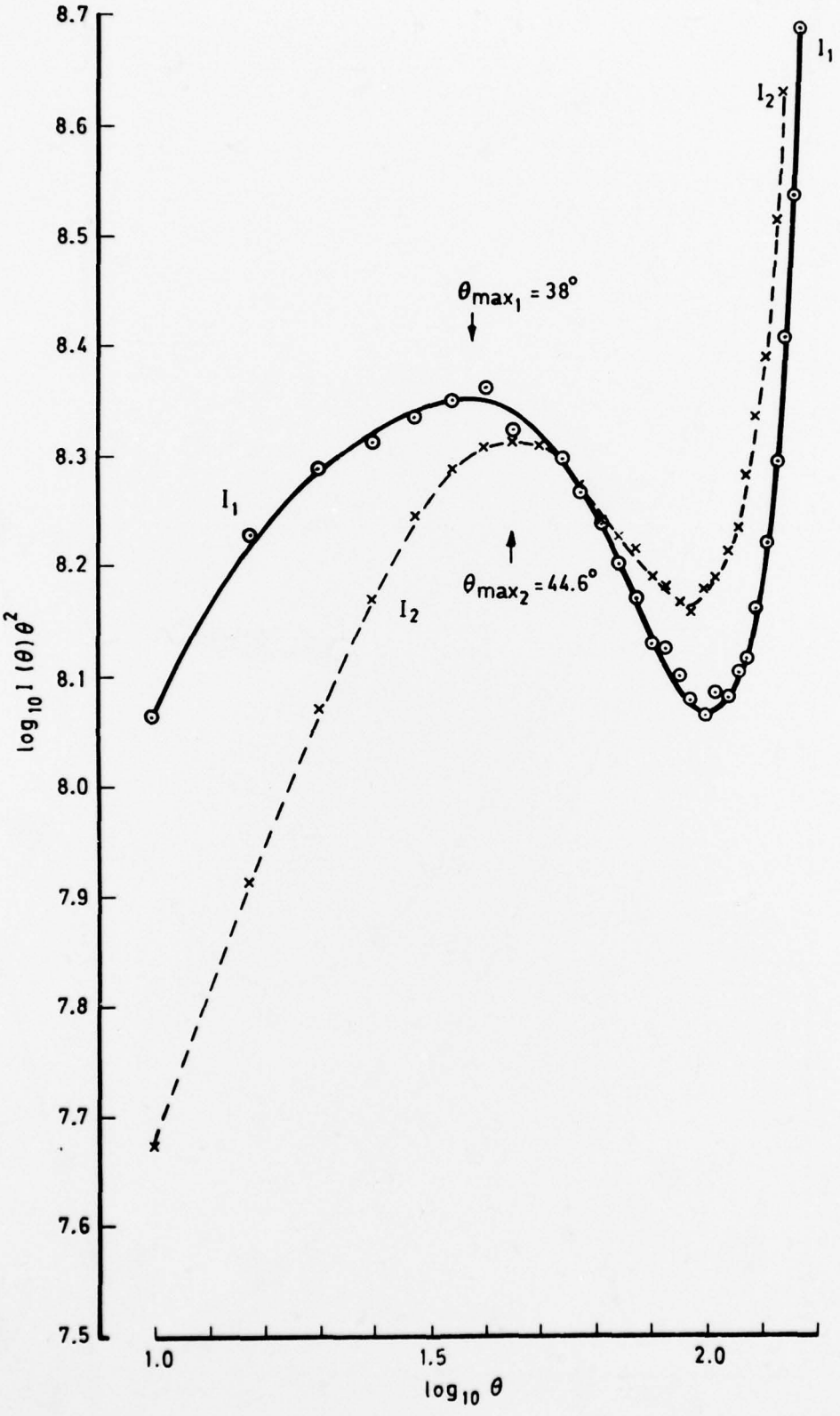

Fig 17 Sloan-type plots for filtered particles

TR 78055

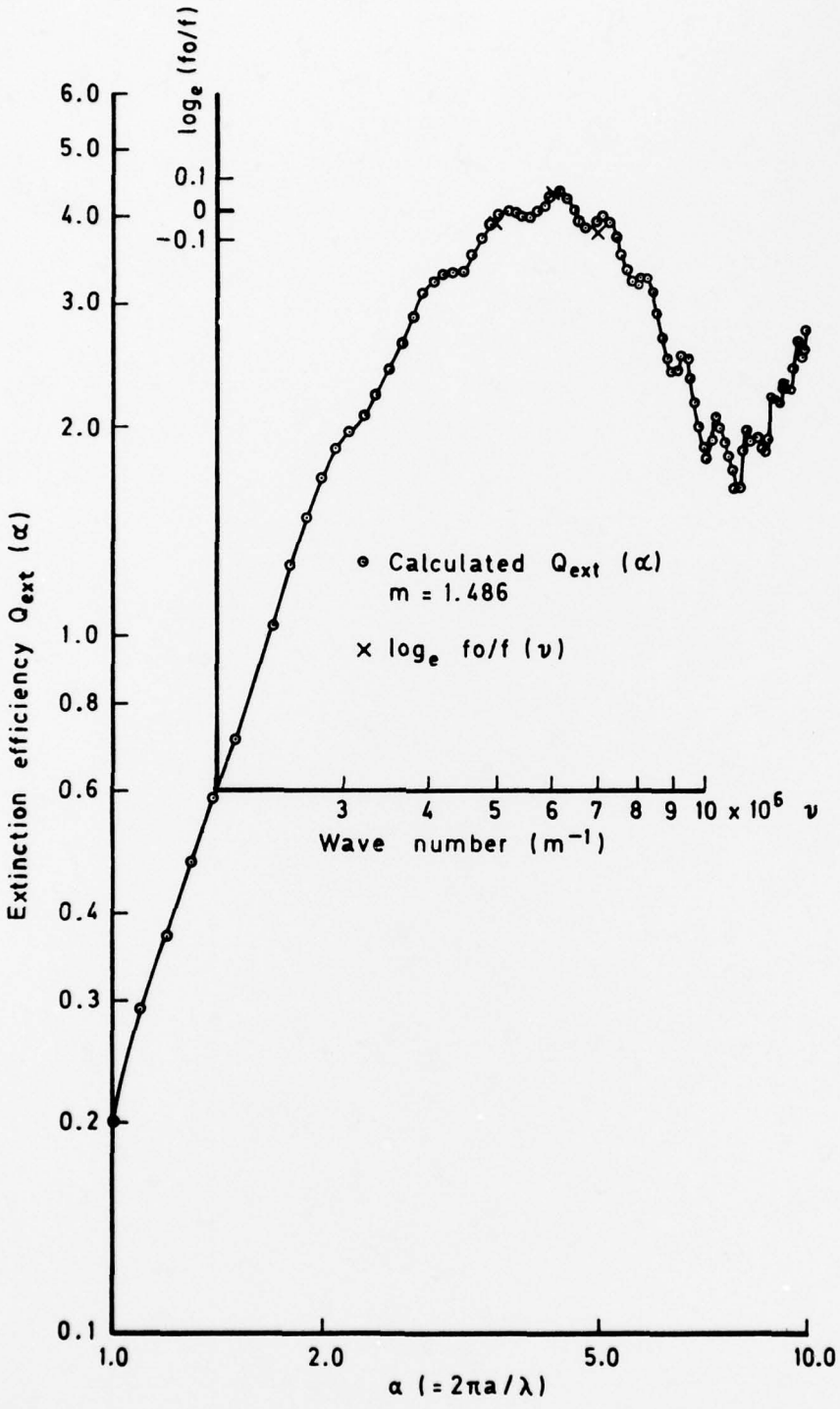

Fig 18 Superimposed plots $Q_{ext}(\alpha)$ and $\log_e(fo/f)/\nu$ for filtered particles

TR 78055